Accepted Manuscript

Raman vibrational dynamics of hydrated ions in the low-frequency spectral region

Ismael A. Heisler, Kamila Mazur, Stephen R. Meech

Please cite this article as: Ismael A. Heisler, Kamila Mazur, Stephen R. Meech, Raman vibrational dynamics of hydrated ions in the low-frequency spectral region, *Journal of Molecular Liquids* (2016), doi: 10.1016/j.molliq.2016.09.066

Raman Vibrational Dynamics of Hydrated Ions in the Low-Frequency Spectral Region

Ismael A. Heisler*, Kamila Mazur and Stephen R. Meech*

School of Chemistry, Norwich Research Park, University of East Anglia, Norwich NR4 7TJ, United Kingdom

*To whom correspondence should be addressed. E-mail: i.heisler@uea.ac.uk,

s.meech@uea.ac.uk

Abstract

The hydration structure of ions in aqueous environments can have a significant influence on their chemical and biological properties. Due to its inherent dynamical character, determination of the hydration shell around dissolved ions has proved challenging, mainly so for cations such as sodium and potassium which form diffuse and dynamic hydrating structures. The low frequency polarized Raman spectrum, as retrieved by time resolved isotropic optical Kerr effect measurements, is sensitive to structural fluctuations and can reveal information about ion-water interactions through their Raman active vibrational modes. Here we study a series of mixtures of sodium, potassium and lithium hydroxide solutions by changing cation concentration pairwise (namely, sodium/potassium or sodium/lithium) while keeping constant the hydroxide concentration. The hydroxide-water hydrogen bond vibration, which produces a well-defined isotropic Raman mode, appears at higher frequencies from the cation-water Raman active vibrations. In addition to previously reported lithium-water low frequency vibrations, clear spectral features could be resolved from the concentration studies and assigned to sodium-water hydration shell vibrations. However, potassium related low frequency spectral features remain elusive. The same method was applied to mixtures of the same cations with a halide anion (chloride) in order to rule out any specific features related to the dissolved hydroxide anion. Comparison between halide and hydroxide measurements confirmed the presence of the cation modes and further revealed a low frequency spectral feature related to hydroxide induced changes in water polarizability.

1. Introduction

The low frequency vibrational spectra of liquid solutions contain important and unique information about solvent dynamics and solute-solvent interactions.[1-4] Characteristic low frequency modes can reveal information about ion hydration, ionic dissociation and ion-pair formation.[5] The understanding of the structure and dynamics of ion hydration is important, especially in the fields of chemistry and biology.[6, 7] For example, many functions in the human body are regulated by ion-water interactions as exemplified by ion channels that are key features in cellular operation.[8] In addition, protein precipitation is regulated by the presence of ions, with some ions being more effective than others (the Hofmeister series) in denaturating proteins.[9] Therefore, it is essential to have a better understanding of the specific interaction mechanisms, interaction strengths and dynamics of hydrated ions in solution.

Ions, as present in aqueous solutions, have been actively investigated through different techniques including Raman spectroscopy, dielectric relaxation spectroscopy (DRS), infrared (IR), neutron diffraction (ND) and X-ray absorption and scattering spectroscopy.[1, 5, 6, 10, 11] The latter techniques such as ND and X-ray are able to provide detailed structural information whereas DRS enables determination of hydration numbers and the association constants for ion pairs in differing conditions, such as solvent shared or separated or contact ion pairs.[5] Recently it was shown that by measuring the isotropic optical Kerr effect (OKE) response of aqueous alkali halide and hydroxide solutions, the hydrogen bond (H-bond) vibration between water and anions could be observed in the time domain.[1, 2] Through a Fourier Transform procedure, it proved possible to recover the low frequency Raman spectrum which showed well-defined modes related to the anion-water H-bond vibration in those solutions. This in-turn permitted the unambiguous determination of some important water-anion H-bond parameters, such as frequency, force constant and dephasing

time. Although our previous focus was on water-anion H-bonds, the effect of the cations was also noted through their electric field effects, namely, by blue shifting the water-anion H-bond vibration frequencies.

The hydration structure of cations in aqueous solutions has attracted great interest within the physical chemistry community. Significant effort has been put into elucidating the hydration structure of sodium (Na^+) and potassium (K^+) cations due to their great physiological importance.[12-14] Molecular dynamics simulations indicated that hydrated cations produce characteristic low frequency Raman vibrational modes, although with lower amplitude when compared to water-anion H-bond vibrations.[15] Indeed early on, we were able to identify clear spectral signatures for doubly and triply charged cations such as calcium, magnesium and aluminium.[1] Nevertheless, singly charged cations did not seem to produce well-defined low frequency modes, the exception being lithium (Li^+) which, due to its strong interaction with water oxygen, presented a clear isotropic vibrational mode in the region around 220 cm^{-1}.[16]

In this work we present a series of measurements intended to identify low frequency vibrational features related to the hydrated cation and also to investigate the effect on those vibrational modes of changing the solute concentration varying the counter-ion. The ultimate objective is to identify and characterise specific features of the hydration shell related to the presence of the singly charged Na^+ and potassium K^+ cations.

2. Experimental

2.1 Materials

Water, salts and hydroxides were of analytical grade (Sigma-Aldrich). The solutions were injected into 2 mm path length fused silica cuvettes through a 0.2 μm micropore filter to

remove any particulate matter. Because of significant contributions of signals from the cell walls to the weak isotropic response, a 2 mm path length cuvettes were selected to ensure that the beams crossed only in the liquid.

2.2 Instrumentation

The experimental setups used were similar to those described in previous publications.[1, 17, 18] Briefly, for the isotropic OKE measurements, the ultrashort pulses were generated in a commercial Kerr-lens mode-locked Ti:Sapphire laser (Micra 10, Coherent). The output had a centre wavelength around 800 nm with 80 nm bandwidth and 800 mW average power. A pair of fused silica prisms was used for compensation of the temporal broadening of pulses directly emitted from the oscillator, and also for precompensation for dispersion due to propagation through the optics used in the experiment. Measuring the autocorrelation at the sample position in a 50 μm BBO crystal revealed typical pulse durations of 20 fs. In order to be able to access all the different third order nonlinear susceptibility elements we worked with a diffractive optic based transient grating spectrometer. We were interested mainly in the isotropic response, for which the probe polarization was aligned parallel with the analysing polarizer and at 54.7^o with respect to the pump (known as the magic angle).[19] The third order nonlinear signal generated in the sample was mixed with the fourth beam (called local oscillator (LO)) from the diffractive optics element to obtain a fully heterodyne detected measurement. The phase between the LO electric field and the signal field was adjusted with a pair of microscope cover slips (200 μm thickness) to an angle of 90° such that the birefringent contribution was accessed.[20]

2.3 Data Interpretation

Measurements of the third order isotropic polarisability relaxation signals were performed in the time domain. The detected signal, *S*(*t*), is a convolution of solution

polarisability response function, $R(t)$ with the instrument response function, $G^{(2)}(t)$ which is the second order autocorrelation of the laser pulses, $S(t) = R(t) \otimes G^{(2)}(t)$.[21] Both single molecule and interaction-induced processes and their cross terms contribute to the observed signal. Further details of OKE spectroscopy can be found elsewhere.[22, 23] The signal $S(t)$ can generally be separated into fast (subpicosecond) and slow (picosecond to nanosecond) contributions. The former typically manifests oscillatory behaviour and contains information about non-diffusive and interaction-induced dynamics, while the latter exhibits monotonic, often non single exponential, relaxation and contains information on diffusive orientational relaxation and H-bond network reorganization.[24] The method has been widely used to probe dynamics in simple liquids, ionic liquids and complex fluids.[25-29]

The dynamics acquired through OKE can be analysed in both time and frequency domain. The frequency domain representation is readily calculated from the Fourier Transform (FT) deconvolution relationship, $FT[S(t)] / FT[G^{(2)}(t)] = D(\omega)$. The imaginary part of $D(\omega)$, $(\mathrm{Im}[D(\omega)])$, contains only information about the nuclear part of the polarisability response.[22] The result is the Raman Spectral Density (RSD), i.e., RSD= Im $[D(\omega)]$.

3. Results and Discussion

Before presenting and discussing salt and hydroxide aqueous solutions it is important to note that the isotropic OKE response is not sensitive to molecular orientational motions. As a consequence it is given mainly by the interaction-induced polarizability response, which may include higher order dipole-induced dipole terms (as first discussed by Mazzacurati et al), in addition to low frequency polarized vibrational modes.[30-34]

As discussed before (and shown in Figure 1a), the pure water isotropic OKE signal decays with a single exponential component with a time constant around 50fs.[1] There is also some evidence that there are even faster relaxation processes at early times which are difficult to capture experimentally and which could be related to quantum effects of the hydrogen atom.[33] More importantly, there are no low frequency modes related to the H-bonded structure present in liquid water (and which produces well defined bands in the anisotropic OKE response) as can be seen in Figure 1b. The isotropic OKE spectrum consists only of a broad featureless band that can be fitted to a combination of a Bucaro-Litovitz (BL) function plus an asymmetric Gaussian (AG) function (details of these fitting functions are presented in reference [35]). The full understanding of the origin of this band lies beyond the scope of this work, and requires further theoretical and molecular dynamics simulations to be fully determined. We know that this band is not affected by isotopic substitution and is insensitive to temperature variations within a region of 268 K to 332 K (unpublished data).

NaCl, is ionized in aqueous solution and the ions are independently hydrated by water molecules. Water molecules form H-bonds with the anions and the water oxygen atom interacts through van der Waals forces with the cations.[6] The symmetry of these new structures might be such that it allows the appearance of polarized Raman active vibrations. Indeed, we reported previously that the hydrated halide anions produce well defined low frequency vibrational modes which are readily recorded by the isotropic OKE measurements.[1] For instance, the hydrated chloride anion produced a polarized band with a frequency around 170 cm^{-1}, similar to the frequency of the H-bond vibration of water molecules in the bulk liquid. Through DFT calculations, it proved possible to determine the solvation structure, which produced polarized modes with frequencies similar to those measured experimentally. Also it was possible to determine the H-bond force constant which turned out to be similar to the force constant of water-water H-bonds. This result underpinned

7

the well-known fact that water accommodates halide anions extremely well into its structure. Those anions hardly produce any alteration to the water dynamical properties. An exception to this rule is the hydroxide anion which forms a significantly stronger H-bond to water.[36] The frequency of the hydration modes of OH^- measured by isotropic OKE experiments was around 280 cm^{-1}, producing an H-bond force constant twice that of water-water H-bonding.

The low frequency Raman modes of singly charged cations were not resolved in our previous measurements. In order to access the presence of such modes we have performed a series of isotropic OKE measurements on mixtures of salts and bases by keeping the concentration of the anion constant but varying the concentration of the cation. Changes in the spectrum are then expected to be due to the solvated cation. Hydroxides are ideal because the OH^- anion produces a relatively high frequency hydration shell mode and, therefore, is not overlapping with the lower frequency region, where the cation modes are expected. Therefore, we present below results for a series of mixtures of NaOH, KOH and LiOH, and then further measurements on NaCl and LiCl mixtures, which are intended to rule out any specific features related to hydroxide anion present in the basic solutions.

3.1 - Sodium and Potassium Hydroxides

In order to illustrate the typical time domain measurements obtained in this work, Figure 2a shows the temporal evolution of the isotropic OKE signal for a 6M NaOH and a 6M KOH aqueous solution. The signal around time zero is due mainly to an electronic contribution (instantaneous laser induced electronic cloud deformation) and is much stronger than the nuclear time evolution that appears after around 50fs.[33] Although the data can be analysed in the time domain, to align with conventional Raman and other low frequency spectroscopies, the signal is presented in the frequency domain in Figure 2b, which is obtained by the Fourier transform procedure outlined above. The results shown in Figure 2b

8

are the corresponding low frequency isotropic Raman OKE spectra for a series of NaOH and KOH mixtures, where one series has a fixed 3M OH^- concentration and the second has a 6M OH^- concentration. The concentration of Na^+ and K^+ cations was varied inversely. The striking feature observable from those measurements is an amplitude increase in the region around 170 cm^{-1}. As the amplitude grows with increasing Na^+ concentration (and decreasing K^+ concentration), the immediate conclusion is that this spectral feature is due to a polarized Raman active mode of hydrated Na^+ ions.

In order to quantify the spectral changes observed in Figure 2, the data were fit to a maximum of three lineshapes, as shown in Figure 3 for the 3M OH^- series: a low frequency (LF) lineshape, an intermediate lineshape, related to the cation, and a high frequency (HF) lineshape related to the OH^- anion. The procedure to fit the data consisted in initially fitting the neat H_2O isotropic spectrum (Figure 1) to a combination of BL and AG functions (as already mentioned above). The same combined function (with parameters fixed to those obtained by fitting neat H_2O) was then used to fit the low frequency region of the Na^+/ K^+/OH^- mixtures by allowing only the LF mode amplitude vary. We had already noticed that this frequency region has a very similar shape to the band measured for pure water, although the amplitude is higher in ionic solutions when compared to neat water; this might be expected given that ions can add a term to the water interaction induced polarizability.[37-40] The HF mode, which is clearly related to the OH^- anion, was fitted to a Gaussian lineshape with the three parameters recovered, i.e. central frequency, bandwidth and amplitude, similar to those already reported, although a better fit was obtained by leaving those parameters float over a small range of values.[36]

By fitting the 3M KOH spectrum first it was found to be necessary to use a third broad AG mode which was added to the LF lineshape (now defined as LF_{AG}) the parameters of which including its amplitude, were kept fixed in all subsequent fittings of the mixture

9

spectra, Importantly, this additional Gaussian was also required in 3M NaOH and was observed to be independent of either Na^+ or K^+ concentrations. Therefore, we assign it to the presence of the OH^- anion in aqueous solution, an assignment which will be confirmed below by measurements performed in NaCl aqueous solutions, where this extra component is absent. We are not sure as to the origin of this additional polarized OH^- induced band and therefore did not try to assign it further. So far the results seem to indicate only a Na^+ related spectral feature and no additional feature related to the presence of K^+. This is consistent with the available literature, where no experimental or theoretical results regarding K^+ can be found.[15, 41]

By using the recovered fitted parameters for the LF_{AG} and HF bands for 3M KOH we then fitted the 3M NaOH spectrum using another AG lineshape whose parameters were left floating in the region of 100 to 200 cm^{-1}. The recovered fit with its components is shown in Figure 3d. The mode that we tentatively assign to the presence of the hydrated sodium cation has a central frequency of 175 cm^{-1} and a bandwidth of 95 cm^{-1}. Its contribution to the total spectrum amounted to 9.5% of the area. The area (A) under the fitted AG lineshape is related to the intensity (I) of the signal, which is directly proportional to the concentration (C) of the scattering species.[42] More precisely, $A \propto I = \delta C$, where δ is the molar intensity coefficient, equivalent to a Raman cross section scattering coefficient. In principle, it is possible to determine the scattering cross section by comparing a given signal to a known reference sample. For the $Na^+/K^+/OH^-$ mixtures, the Na^+ mode had its central frequency and bandwidth fixed and the amplitude was left floating. The obtained fits are very good (Figure 3b,c). It is now possible to calculate the fitted mode area contribution and plot it against the Na^+ cation concentration in the pure and mixture solutions. The result is shown in Figure 4a. Clearly, the Na^+ cation contribution increases linearly with increasing concentration as shown by the linear fit (black line). This is good evidence that the proposed mode is indeed related to the

10

Na$^+$ cation. The LF$_{AG}$ band recovered from fitting the 3M and 6M Na$^+$/K$^+$/OH$^-$ mixtures and for pure water is shown in Figure 4b. There is a small variation mainly because only the low frequency water spectrum was allowed to change amplitude. But within the experimental uncertainty they are all equal at each OH$^-$ concentration. It is worth noticing the amplitude enhancement when compared to the band recovered for pure water, and that the amplitude increases with increasing OH$^-$ concentration.

There is good evidence in the literature that the Na$^+$ cation in aqueous solutions is hydrated by at least four water molecules, but most likely forms a penta-hydrate structure as suggested by X-ray measurements and neutron diffraction studies, even though these studies also revealed that the hydration sphere is rather malleable.[15, 43, 44] Further, molecular dynamics calculations also support the most stable hydrated Na$^+$ cation structure as [Na(OH$_2$)$_5$]$^+$. Therefore a possible assignment for the intermediate isotropic OKE mode, revealed in Figures 2 and 3, is the Na$^+$---OH$_2$ stretching mode of the hydrated [Na(OH$_2$)$_5$]$^+$ structure. The experimentally determined frequency for this mode agrees fairly well with experimental and theoretical literature reports. For instance, molecular dynamics calculations by Bour et al found a mode at around 172 cm^{-1} for the fairly polarized hydrated Na$^+$---OH$_2$ stretching mode.[15] Further calculations by the same group compared the amplitudes for the Na$^+$/ Mg^{2+} /Ca^{2+}---OH$_2$ stretching vibrational modes, concluding that the Na$^+$---OH$_2$ mode had a smaller amplitude compared to the doubly charged cations. We showed previously that the measured modes for doubly charged cations in aqueous solutions such as CaCl$_2$ and MgCl$_2$ were readily observed and agreed fairly well with the frequencies calculated by Bour et al.[1] The present work shows further agreement for Na$^+$ cations. Early experimental work by Michaelian and Moskovits proposed a tetrahedral [Na(OH$_2$)$_4$]$^+$ hydration structure responsible for producing a polarized low frequency vibrational mode at 172 cm^{-1}.[45] Subsequently Rudolph performed Raman measurements on aqueous NaCH$_3$CO$_2$ solutions

and assigned a polarized band at 189 cm^{-1}, present in the isotropic Raman spectrum, to the Na$^+$---OH$_2$ stretching vibration of a [Na(OH$_2$)$_5$]$^+$.[46] Further calculations that take into account our present findings and earlier results from other techniques could provide details about the exact structure hydrating the Na$^+$ cation in aqueous solution. Finally, our results show that K$^+$ does not produce any detectable low frequency vibrational mode, most likely due to the fact that this ion is not able to form a stable and long lived hydration structure.

3.2 - Lithium and Sodium Hydroxides

To test the consistency of our results against a broader range of aqueous hydroxide solutions we carried out another series of measurements with mixtures of LiOH and NaOH solutions. Figure 5 shows spectra for single and mixtures of aqueous solutions of LiOH and NaOH together with their best fit. The fitting procedure was similar to the one applied to NaOH and KOH mixtures discussed above, i.e., a LF$_{AG}$ band, composed of a water mode plus an (OH$^-$ induced) broad AG band (see above), a HF band accounting for the hydrated OH$^-$ mode plus intermediate bands accounting for Li$^+$ and Na$^+$---OH$_2$ stretching vibrations. We started by fitting the 3M LiOH solution and therefore determined the hydrated Li$^+$---OH$_2$ stretching vibration. The recovered frequency was 222 cm^{-1} and the bandwidth 85 cm^{-1}. The contribution to the total spectrum was 22% of the total area. The central frequency is lower but in general agreement with previous experimental and theoretical results.[1, 16] This mode was fixed in the subsequent fittings of the spectra resulting from the mixtures of LiOH and NaOH, as shown in Figure 5. As the concentration of Na$^+$ increases in the mixtures it is necessary to add some amplitude due to the appearance of Na$^+$---OH$_2$ mode in order to be able to fit the data properly. In these fittings, the only parameter left floating, in regards to the Na$^+$---OH$_2$ mode, was its amplitude. Again, by calculating the area contribution due to the Na$^+$---OH$_2$ mode and Li$^+$---OH$_2$ mode and plotting them against their respective concentrations one obtains linear dependencies, as shown in Figure 6a and b, respectively.

12

It is interesting, at this point, to summarize the data recovered by fitting the hydroxide series for different cations and different hydroxide concentrations. Figure 4b presents the LF_{AG} recovered spectra, whereas Figure 7a shows the OH^----H_2O stretching vibration mode, and Figure 7b shows the area due to the Na^+---OH_2 stretching vibration as a function of concentration for all the fitted spectra, i.e., LiOH/NaOH and KOH/NaOH. The recovered LF_{AG} bands are very clearly dependent on the OH^- concentration. However the LF_{AG} band is insensitive to the character and concentration of the cations present in the solution. The area associated with the OH^----H_2O stretching vibration mode scales with the OH^- anion concentration in the solution and the same happens to the mode assigned to the hydrated cation, i.e., the Na^+---OH_2 stretching vibration mode. By summarizing the results for the entire series of mixtures containing Na^+ cations, the fitted mode area scales linearly over a broad concentration range as shown in Figure 7b providing further evidence that the mode at 170 cm^{-1} is indeed related to a Na^+---OH_2 stretching vibration. The linear concentration dependence also proves that there is no evidence for ion-pair formation affecting the spectra, at least for the typical concentrations studied here.

3.3 - Lithium and Sodium Chloride

The final dataset consists of a series of mixtures of alkali halide aqueous solutions. The time domain experimental data are shown in Figure 8a for 6M LiCl and 6M NaCl, and in Figure 8b the corresponding isotropic OKE spectra obtained by Fourier transform are shown for all mixtures. By performing measurements in aqueous salt solutions with constant chloride ion concentration the objective is to check for any specific effects or features related to the dissolved OH^- anion in the measurements above. Even though the recovery of the Na^+---OH_2 stretching mode becomes more problematic (because the hydrated Cl^----HOH anion also produces a band in the region of 170 cm^{-1})[1, 47] it is still possible to obtain

detailed information regarding specific low frequency modes related to hydrated cations and anions.

As shown in Figure 8b, salient features are the appearance of a shoulder at around 230 cm^{-1} and a decrease in the overall amplitude of the spectra by increasing Na^+ /decreasing Li^+ concentration. The first feature can be explained by the appearance of a mode related to the Li^+---OH_2 stretching vibration that is already known to produce a contribution in this spectral region (see above); consistent with this, the amplitude of this mode grows as Li^+ concentration increases. The latter feature, the decreasing amplitude, can be explained by the disappearance of the Na^+---OH_2 stretching vibration mode as the Na^+ concentration decreases.

A fitting procedure similar to that described above was applied and the results are shown in Figure 9. Briefly, the LF mode, determined by fitting pure water (Figure 1) whose only floating parameter was its amplitude, and three AG lineshapes accounting for contributions related to the Cl^----HOH, Na^+---OH_2 and Li^+---OH_2 stretching vibrations were included in the fit. It was not necessary to make use of an intermediate broad band as was the case for mixtures containing OH^-, consistent with the assignment of this component in LF_{AG} to a specific interaction mediated by the hydrated hydroxide anion. The parameters for the Gaussian mode related to the Cl^----HOH stretching vibration were left floating to account for a frequency shift observed when the positive charge density increases in the solution. This is the case when the Li^+/ Na^+ concentration ratio increases in the solutions.[1] The hydrated Cl^----HOH stretching frequency increased from 168 cm^{-1} for the 3M NaCl solution up to 175 cm^{-1} for the 3M LiCl solution. The bandwidth did not change significantly, staying around 110 cm^{-1}. Those values are in good agreement with our previous data.[1] Due to a significant overlap with the Cl^----HOH stretching contribution, the mode related to the Na^+---OH_2 vibration contribution had its central frequency and bandwidth fixed at the values determined

14

previously for the hydroxide series fitting, above. The contribution related to the Li^+---OH_2 stretching vibration produced a frequency around 240 cm^{-1} which is slightly higher than the value recovered for the hydroxide solutions. On the other hand the recovered amplitude for this contribution was lower for the salt solution when compared to the hydroxide solutions, however it still scaled linearly with Li^+ concentration, as shown in Figure 10.

Interestingly, Figure 10 also shows that the Li^+---OH_2 mode amplitude variation with Li^+ is stronger for the hydroxide solutions when compared to halide solution. As discussed earlier, the linear fit slope of the area versus concentration is related to the Raman cross section. This result could therefore mean that the hydrated cation scattering cross section is smaller in solutions containing Cl^- anion, compared to solutions containing OH^- anions. However one cannot discard the possibility of amplitude interplay between the different fitted components, given that there is a significant overlap between the different contributions. Finally, the recovered central frequencies, bandwidths and intensities for the various hydrated cation and anion isotropic OKE vibrational spectra studied in this work are summarized in Table I.

4. Conclusions

In this work we presented and discussed results regarding the low frequency isotropic OKE measurements in a series of salt and hydroxide aqueous solutions. Specifically, by performing measurements on mixtures of KOH/NaOH solutions we have identified a spectral feature around 175 cm^{-1} which was assigned to a Na^+---OH_2 stretching vibrational mode, possibly arising in the previously proposed penta-hydrated $[Na(OH_2)_5]^+$ structure. No evidence was found for the presence of Raman activity in the isotropic spectrum due to hydrated K^+ in solution. Concentration dependent measurements showed a linear dependence of the proposed Na^+---OH_2 mode amplitude with Na^+ concentration in solution.

Confirmation of the presence of the Na$^+$ hydration shell mode was obtained by further measurements on mixtures of LiOH/NaOH as well as on mixtures of LiCl/NaCl. The latter measurement proved that the spectral feature at 175 cm^{-1} was not related to specific hydroxide ion interactions.

Further findings were that the presence of ions in solution also affects the LF band, usually assigned to the water interaction-induced response. A significant amplitude enhancement of the water LF mode was observed when hydroxide ions are dissolved in water, as shown in Figure 4b, pointing to the possibility of a hydroxide-water specific interaction, accounted for here in the LF$_{AG}$ lineshape. All these results can be tested in detailed molecular dynamics calculations which, by their turn in combination with other experimental results, can shed light on the hydrated structures present in ionic aqueous solutions, and further elucidate the specific interactions underlying the important biological activity of dissolved Na$^+$ and K$^+$ ions in aqueous environments.

16

Table I

	Central Frequency (cm^{-1})	Bandwidth (cm^{-1})	Intensity (% of total area[1])
Li^+---OH_2	222	85	22
Na^+--- OH_2	175	95	10
Cl^----HOH	168	107	32
OH^----HOH	260	110	31

Summary of recovered central frequencies, bandwidths and intensities for the cation related (Na^+---OH_2 and Li^+---OH_2) and anion related (Cl^----HOH and OH^----HOH) stretching vibration contributions to the isotropic OKE signal.

[1] The total area of the corresponding neat solution, i.e., for Li^+---OH_2 it is LiOH, for Na^+---OH_2 it is NaOH, Cl^----HOH it is either LiCl of NaCl and for OH^----HOH it is either NaOH or LiOH.

Figure Captions

Figure 1. Pure water isotropic OKE data (a) in time domain and (b) its corresponding spectrum. In (b) the spectral density (vertical axis) is obtained from the imaginary part of the Fourier transform of the OKE signal divided by the measured autocorrelation at the sample position.

Figure 2. (a) Temporal evolution of the isotropic OKE signal for a 6M NaOH and a 6M KOH aqueous solution. (b) Low frequency isotropic OKE spectra for a series of NaOH and KOH mixtures where one series has a fixed 3M OH^- concentration and the second series has a 6M OH^- concentration.

Figure 3. Low frequency isotropic OKE spectra and corresponding total fit plus fitting components for (a) 3M KOH, (b) 2M KOH + 1M NaOH, (c) 1M KOH + 2M NaOH and (d) 3M NaOH. The fitting components that appear on the graphs such as LF_{AG} (low frequency + antisymmetric Gaussian) are described in the text.

Figure 4. (a) Area under the curve fitted to the contribution corresponding to the Na^+---OH_2 stretching vibrational mode as a function of Na^+ concentration in the Na^+/ K^+/OH^- mixtures. (b) LF band fitted to the neat H_2O, and to the Na^+/ K^+/OH^- mixtures containing 3M OH^- and another series containing 6M OH^-.

Figure 5. Low frequency isotropic OKE spectra and corresponding total fit plus fitting components for (a) 3M LiOH, (b) 2M LiOH + 1M NaOH, (c) 1M LiOH + 2M NaOH and (d) 3M NaOH.

Figure 6. (a) Area under the curve fitted to the contribution corresponding to the Na^+---OH_2 stretching vibrational mode as a function of Na^+ concentration in the Na^+/ K^+/OH^- mixtures containing 3M OH^-. (b) Area under the curve fitted to the contribution corresponding to the

Li$^+$---OH$_2$ stretching vibrational mode as a function of Li$^+$ concentration in the Na$^+$/ Li$^+$/OH$^-$ mixtures containing 3M OH$^-$.

Figure 7. Graphs summarizing fitting results. (a) Fitted Gaussian modes corresponding to the OH$^-$---HOH stretching vibrational mode for the Na$^+$/ K$^+$/OH$^-$ mixtures containing 3M OH$^-$ as well as 6M OH$^-$. (b) Area under the curve fitted to the contribution corresponding to the Na$^+$---OH$_2$ stretching vibrational mode as a function of Na$^+$ concentration for all the Na$^+$/ Li$^+$/OH$^-$ and Na$^+$/ K$^+$/OH$^-$ mixtures.

Figure 8. (a) Temporal evolution of the isotropic OKE signal for a 6M NaCl and a 6M LiCl aqueous solution. (b) Low frequency isotropic OKE spectra for a series of NaCl and LiCl mixtures containing a fixed 3M Cl$^-$ concentration.

Figure 9. Low frequency isotropic OKE spectra and corresponding total fit plus fitting components for (a) 3M LiCl, (b) 2M LiCl + 1M NaCl, (c) 1M LiCl + 2M NaCl and (d) 3M NaCl.

Figure 10. Area under the curve fitted to the contribution corresponding to the Li$^+$---OH$_2$ stretching vibrational mode as a function of Li$^+$ concentration in the Na$^+$/ Li$^+$/OH$^-$ mixtures containing 3M OH$^-$ (blue squares) and for Na$^+$/ Li$^+$/Cl$^-$ mixtures containing 3M Cl$^-$ (red circles).
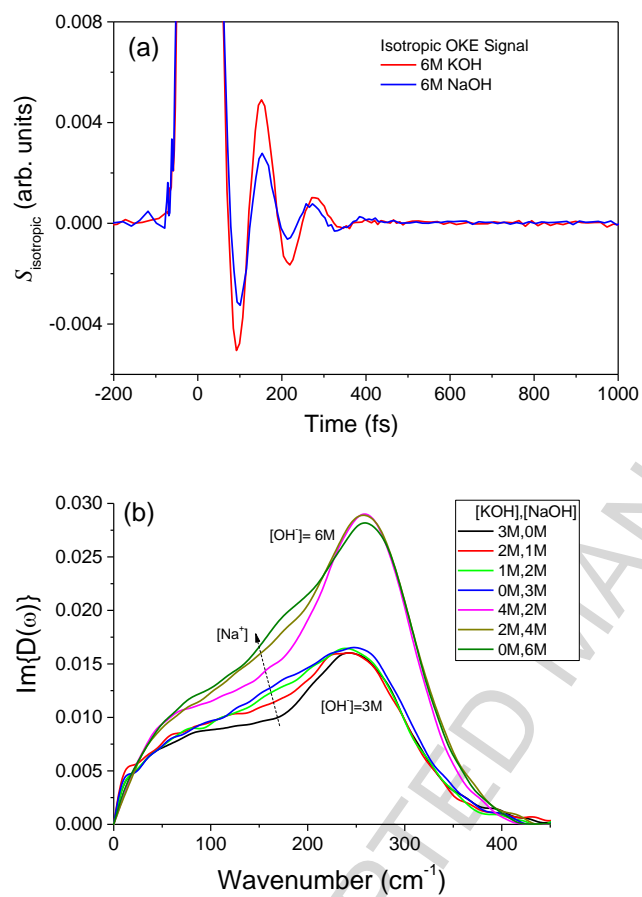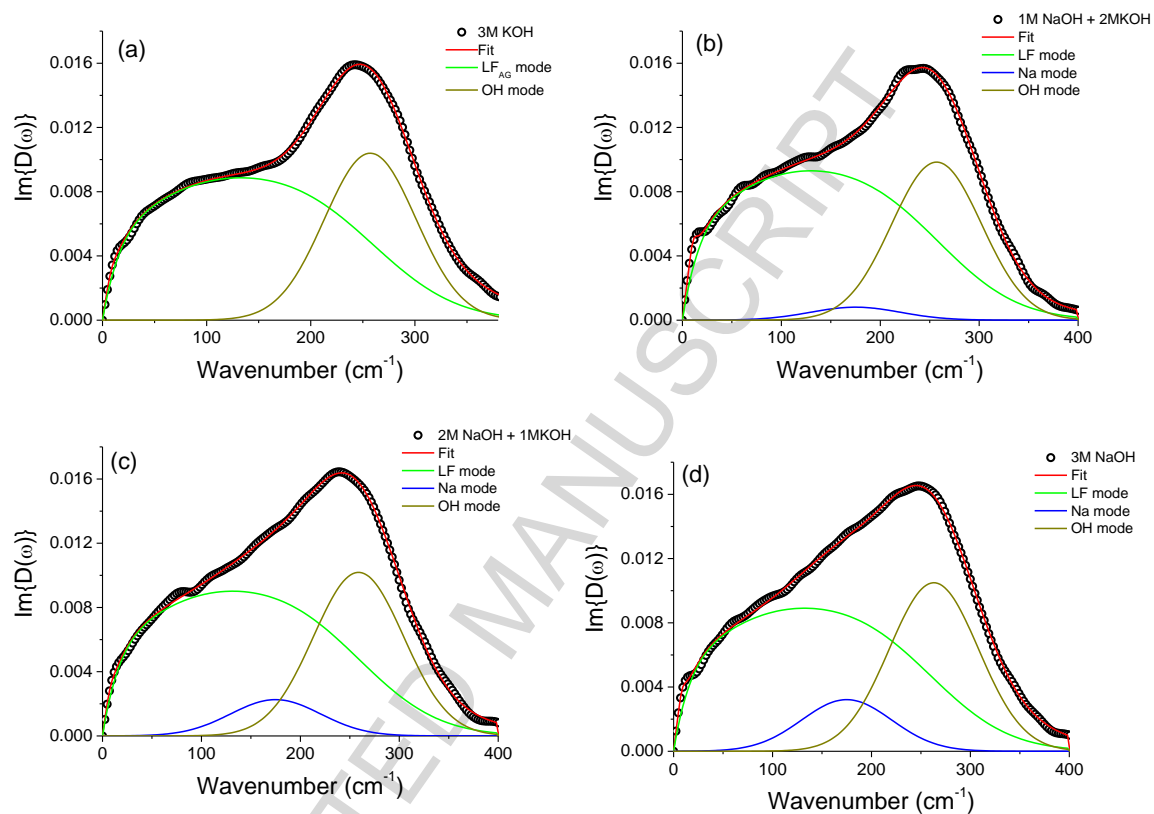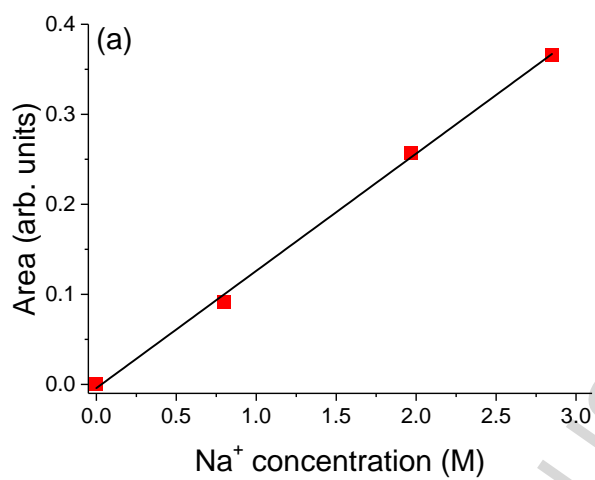
Figure 1
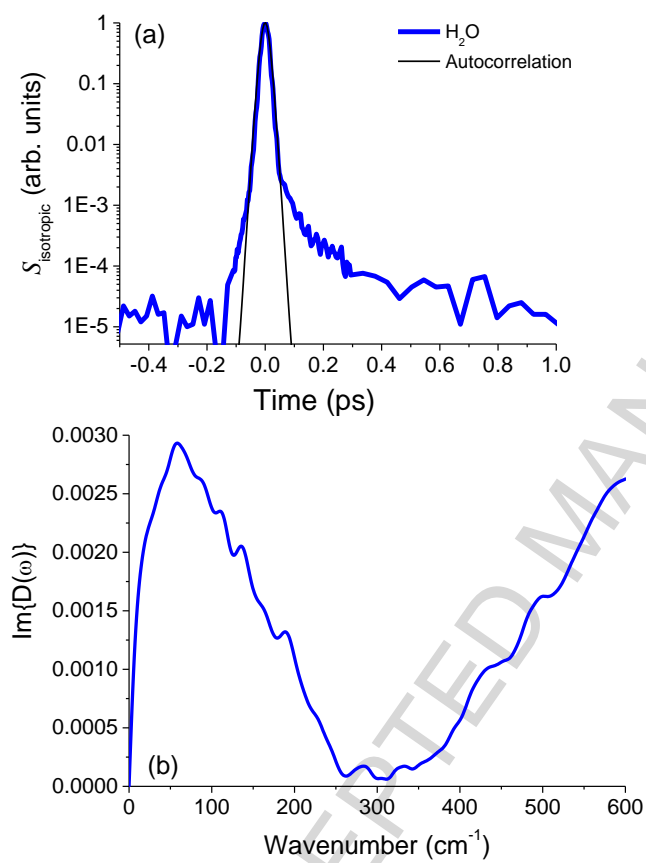
Figure 2

Figure 3

Figure 4
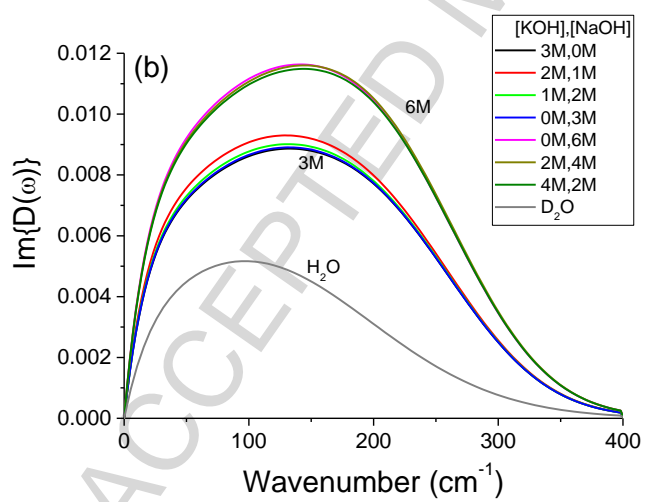
Figure 5
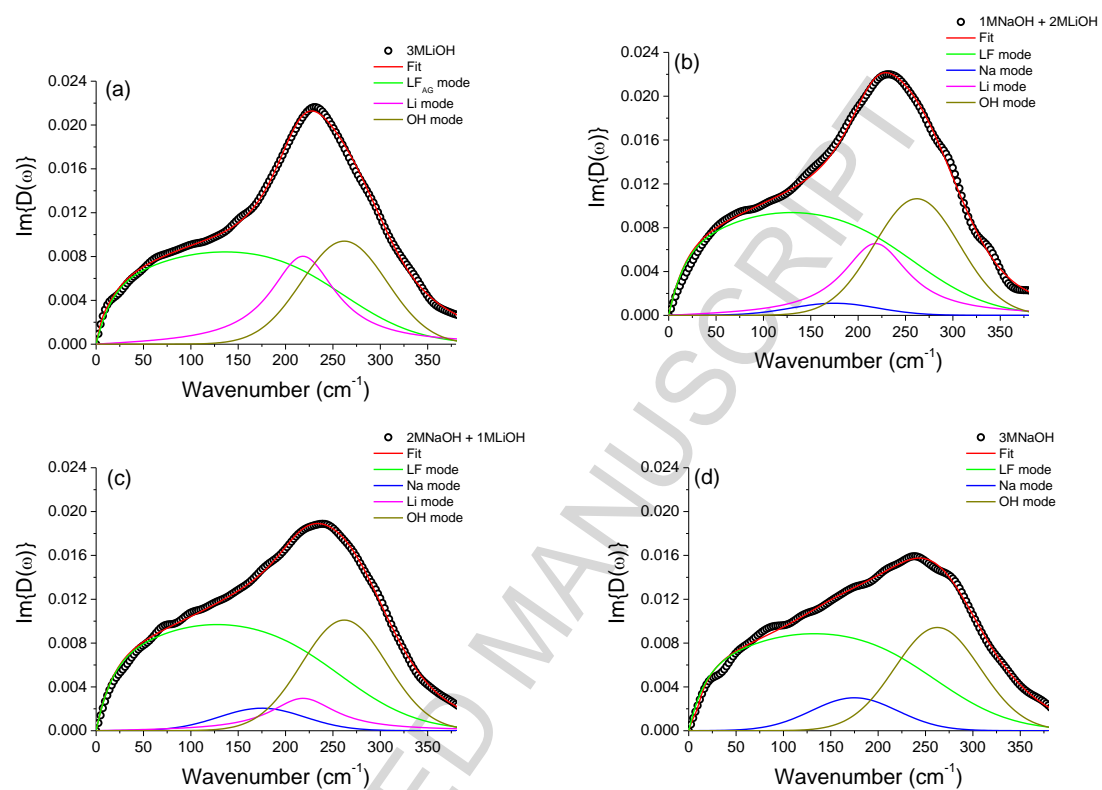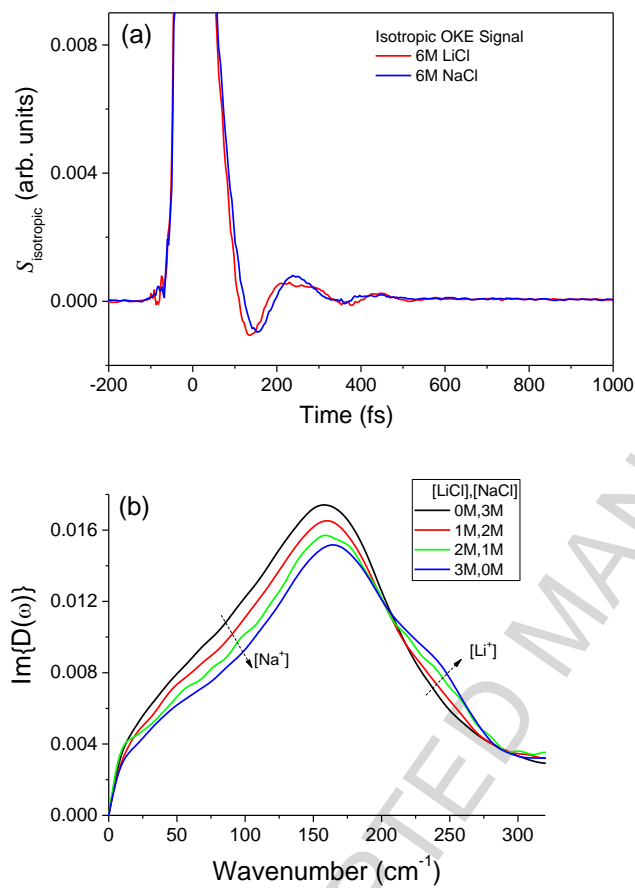
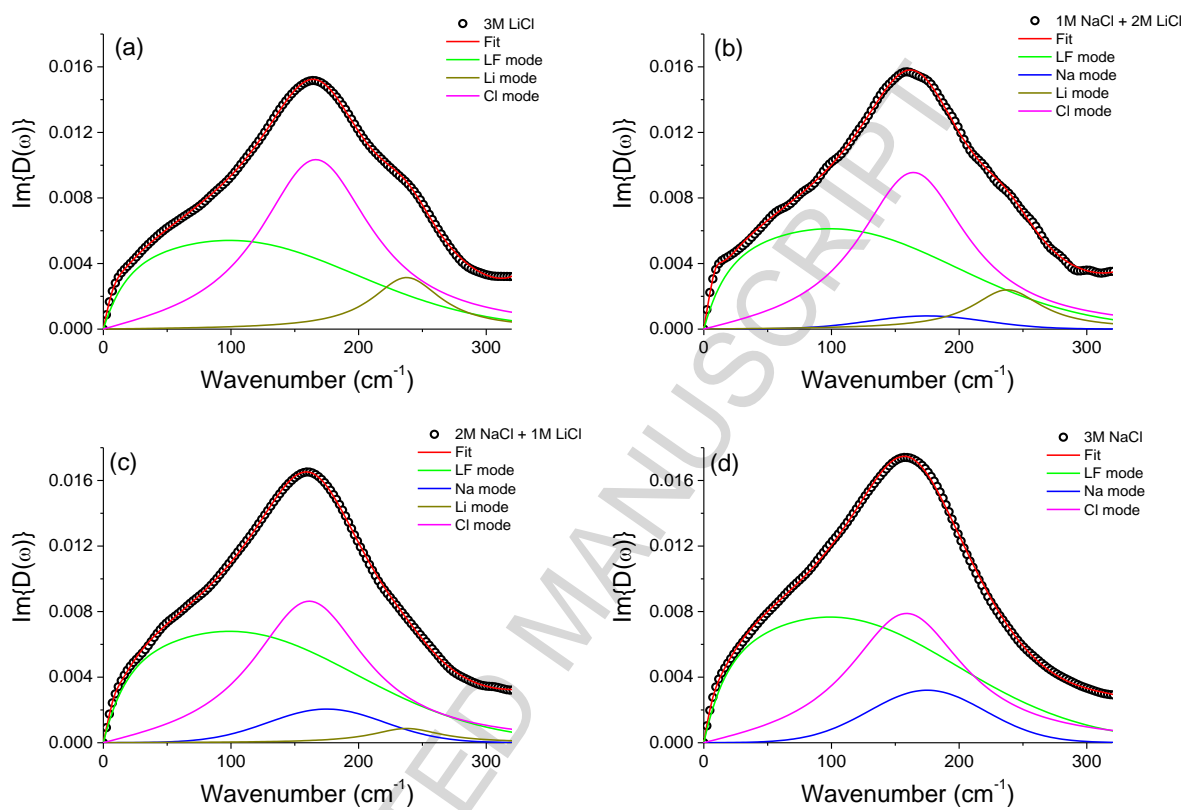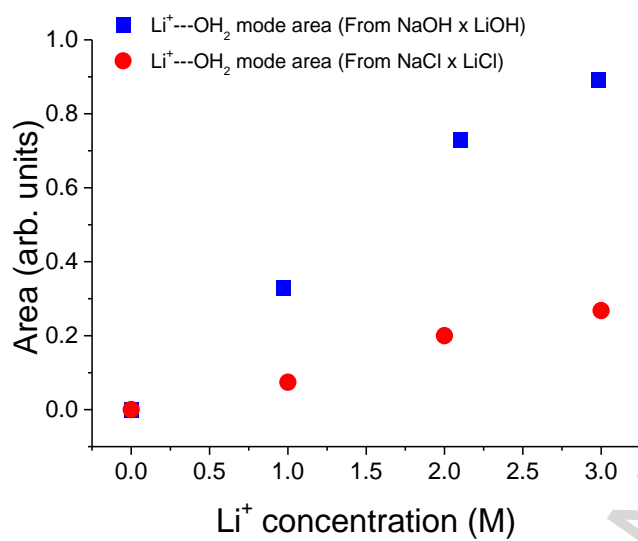**Figure 6**
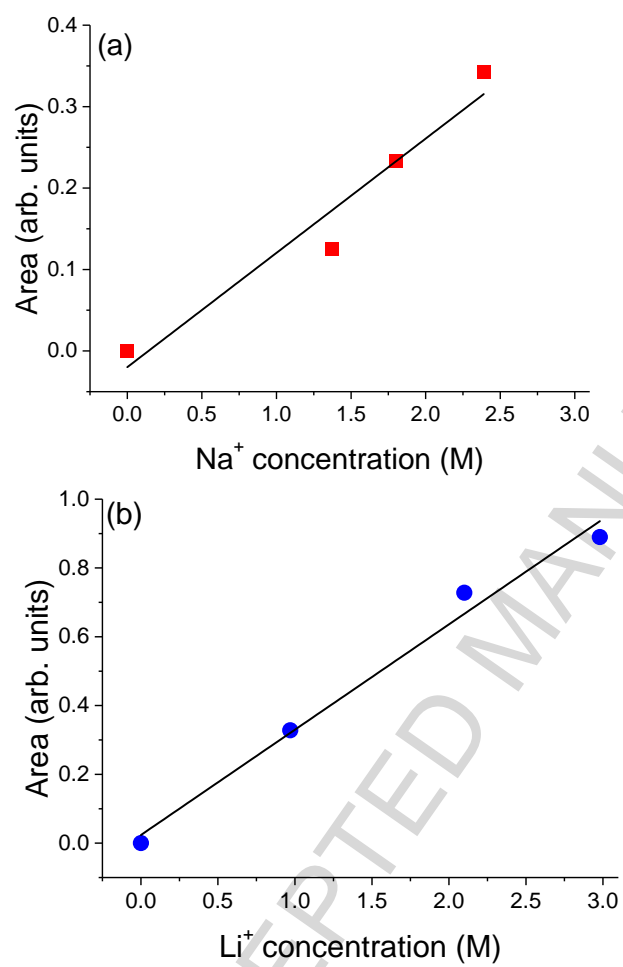
Figure 7
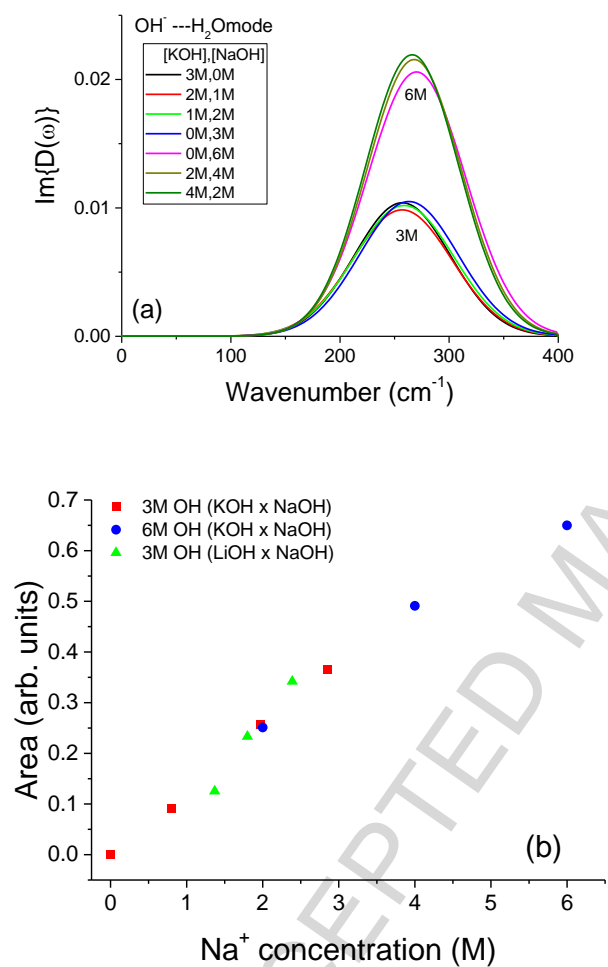
Figure 8

Figure 9

Figure 10

References

[1] I.A. Heisler, K. Mazur, S.R. Meech, Low-Frequency Modes of Aqueous Alkali Halide Solutions: An Ultrafast Optical Kerr Effect Study, J. Phys. Chem. B 115 (2011) 1863-1873.

[2] I.A. Heisler, S.R. Meech, Low-Frequency Modes of Aqueous Alkali Halide Solutions: Glimpsing the Hydrogen Bonding Vibration, Science 327 (2010) 857-860.

[3] S. Funkner, G. Niehues, D.A. Schmidt, M. Heyden, G. Schwaab, K.M. Callahan, D.J. Tobias, M. Havenith, Watching the Low-Frequency Motions in Aqueous Salt Solutions: The Terahertz Vibrational Signatures of Hydrated Ions, J. Am. Chem. Soc. 134 (2012) 1030-1035.

[4] W.W. Rudolph, G. Irmer, Raman spectroscopic studies and DFT calculations on NaCH3CO2 and NaCD3CO2 solutions in water and heavy water, Rsc Adv 5 (2015) 21897-21908.

[5] R. Buchner, G. Hefter, Interactions and dynamics in electrolyte solutions by dielectric spectroscopy, Phys. Chem. Chem. Phys. 11 (2009) 8984-8999.

[6] Y. Marcus, Effect of Ions on the Structure of Water: Structure Making and Breaking, Chem. Rev. 109 (2009) 1346-1370.

[7] K.D. Collins, G.W. Neilson, J.E. Enderby, Ions in water: Characterizing the forces that control chemical processes and biological structure, Biophys. Chem. 128 (2007) 95-104.

[8] I. Restrepo-Angulo, A. De Vizcaya-Ruiz, J. Camacho, Ion channels in toxicology, J. Appl. Toxicol. 30 (2010) 497-512.

[9] K.D. Collins, M.W. Washabaugh, The Hofmeister Effect and the Behavior of Water at Interfaces, Q. Rev. Biophys. 18 (1985) 323-422.

[10] H. Ohtaki, T. Radnai, Structure and Dynamics of Hydrated Ions, Chem. Rev. 93 (1993) 1157-1204.

[11] T. Petit, K.M. Lange, G. Conrad, K. Yamamoto, C. Schwanke, K.F. Hodeck, M. Dantz, T. Brandenburg, E. Suljoti, E.F. Aziz, Probing ion-specific effects on aqueous acetate solutions: Ion pairing versus water structure modifications, Struct. Dyn. 1 (2014) 034901.

[12] P. Lo Nostro, B.W. Ninham, Hofmeister Phenomena: An Update on Ion Specificity in Biology, Chem. Rev. 112 (2012) 2286-2322.

[13] J. Mahler, I. Persson, A Study of the Hydration of the Alkali Metal Ions in Aqueous Solution, Inorg. Chem. 51 (2012) 425-438.

[14] A. Bankura, V. Carnevale, M.L. Klein, Hydration structure of salt solutions from ab initio molecular dynamics, J. Chem. Phys. 138 (2013) 014501.

[15] J. Kapitan, M. Dracinsky, J. Kaminsky, L. Benda, P. Bour, Theoretical Modeling of Magnesium Ion Imprints in the Raman Scattering of Water, J. Phys. Chem. B 114 (2010) 3574-3582.

[16] W. Rudolph, M.H. Brooker, C.C. Pye, HYDRATION OF LITHIUM ION IN AQUEOUS-SOLUTION, J. Phys. Chem. 99 (1995) 3793-3797.

[17] I.A. Heisler, S.R. Meech, Low-frequency isotropic and anisotropic Raman spectra of aromatic liquids, J. Chem. Phys. 132 (2010) 174503.

[18] I.A. Heisler, S.R. Meech, Polarization-Resolved Ultrafast Polarizability Relaxation in Polar Aromatic Liquids, J. Phys. Chem. B 112 (2008) 12976-12984.

[19] J.R. Lakowicz, Principles of Fluorescence Spectroscopy, Third Edition ed., Springer-Verlag New York Inc., New York, 2006.

[20] G.D. Goodno, G. Dadusc, R.J.D. Miller, Ultrafast heterodyne Detected Transient Grating Spectropscopy Using Diffratctive Optics, J. Opt. Soc. Am. B 15 (1998) 1791 - 1794.

[21] N.A. Smith, S.R. Meech, Optically heterodyne Detected Optical Kerr Effect (OHD-OKE): Application in Condensed phase dynamics., Int. Rev. Phys. Chem. 21 (2002) 75-100.

[22] W.T. Lotshaw, D. McMorrow, N. Thantu, J.S. Melinger, R. Kitchenham, Intermolecular Vibrational Coherence In Molecular Liquids, J. Raman Spectrosc. 26 (1995) 571-583.

[23] N.A. Smith, S.R. Meech, Optically-heterodyne-detected optical Kerr effect (OHD-OKE): applications in condensed phase dynamics, International Reviews in Physical Chemistry 21 (2002) 75-100.

[24] D. McMorrow, W.T. Lotshaw, G.A. Kenneywallace, Femtosecond Optical Kerr Studies on the Origin of the Nonlinear Responses in Simple Liquids, Ieee Journal of Quantum Electronics 24 (1988) 443-454.

[25] Q. Zhong, J.T. Fourkas, Optical Kerr Effect Spectroscopy of Simple Liquids, J. Phys. Chem. B 112 (2008) 15529-15539.

[26] H. Shirota, T. Fujisawa, H. Fukazawa, K. Nishikawa, Ultrafast Dynamics in Aprotic Molecular Liquids: A Femtosecond Raman-Induced Kerr Effect Spectroscopic Study, Bull. Chem. Soc. Jpn. 82 (2009) 1347-1366.

[27] G. Giraud, C.M. Gordon, I.R. Dunkin, K. Wynne, The effects of anion and cation substitution on the ultrafast solvent dynamics of ionic liquids: A time-resolved optical Kerr-effect spectroscopic study, J. Chem. Phys. 119 (2003) 464-477.

[28] N.T. Hunt, A.A. Jaye, A. Hellman, S.R. Meech, Ultrafast dynamics of styrene microemulsions, polystyrene nanolatexes, and structural analogues of polystyrene, J. Phys. Chem. B 108 (2004) 100-108.

[29] N.T. Hunt, A.A. Jaye, S.R. Meech, Ultrafast dynamics in microemulsions: Optical Kerr effect study of the dispersed oil phase in a carbon disulride- dodecyltrimethylammonium bromide-water microemulsion, J. Phys. Chem. B 107 (2003) 3405-3418.

[30] A. Desantis, M. Sampoli, V. Mazzacurati, M.A. Ricci, RAMAN-SPECTRA OF WATER IN THE TRANSLATIONAL REGION, Chem. Phys. Lett. 133 (1987) 381-384.

[31] A. Desantis, R. Frattini, M. Sampoli, V. Mazzacurati, M. Nardone, M.A. Ricci, G. Ruocco, RAMAN-SPECTRA OF WATER IN THE TRANSLATIONAL AND LIBRATIONAL REGIONS .1. STUDY OF THE DEPOLARIZATION RATIO, Mol. Phys. 61 (1987) 1199-1212.

[32] V. Mazzacurati, M.A. Ricci, G. Ruocco, M. Nardone, ISOTROPIC INDUCED SCATTERING IN LIQUID H2S, Mol. Phys. 50 (1983) 1083-1087.

[33] C.J. Fecko, J.D. Eaves, A. Tokmakoff, Isotropic and Anisotropic Raman Scattering from Molecular Liquids Measured by Spatially Masked Optical Kerr Effect Spectroscopy, J. Chem. Phys. 117 (2002) 1139-1154.

[34] M.D. Elola, B.M. Ladanyi, Computational study of structural and dynamical properties of formamide-water mixtures, J. Chem. Phys. 125 (2006) 184506.

[35] K. Mazur, I.A. Heisler, S.R. Meech, Ultrafast Dynamics and Hydrogen-Bond Structure in Aqueous Solutions of Model Peptides, J. Phys. Chem. B 114 (2010) 10684-10691.

[36] I.A. Heisler, K. Mazur, S.R. Meech, Hydroxide Hydrogen Bonding: Probing the Solvation Structure through Ultrafast Time Domain Raman Spectroscopy, Journal of Physical Chemistry Letters 2 (2011) 1155-1160.

[37] M.R. Harpham, N.E. Levinger, B.M. Ladanyi, An investigation of water dynamics in binary mixtures of water and dimethyl sulfoxide, J. Phys. Chem. B 112 (2008) 283-293.

[38] M.D. Elola, B.M. Ladanyi, Intermolecular polarizability dynamics of aqueous formamide liquid mixtures studied by molecular dynamics simulations, J. Chem. Phys. 126 (2007) 084504.

[39] B.M. Ladanyi, M.D. Elola, Polarizability anisotropy dynamics in water-formamide mixtures, in: T. Simos, G. Maroulis (Eds.), Recent Progress in Computational Sciences and Engineering, Vols 7a and 7b2006, pp. 1107-1112.

[40] M.D. Elola, B.M. Ladanyi, Molecular dynamics study of polarizability anisotropy relaxation in aromatic liquids and its connection with local structure, J. Phys. Chem. B 110 (2006) 15525-15541.

[41] W.W. Rudolph, G. Irmer, Raman and infrared spectroscopic investigations on aqueous alkali metal phosphate solutions and density functional theory calculations of phosphate-water clusters, Appl. Spectrosc. 61 (2007) 1312-1327.

[42] J.B. Ng, H.F. Shurvell, Application of Factor-Analysis and Band Contour Resolution Techniques to the Raman-Spectra of Acetic-Acid in Aqueous-Solution, J. Phys. Chem. 91 (1987) 496-500.

[43] S. Varma, S.B. Rempe, Coordination numbers of alkali metal ions in aqueous solutions, Biophys. Chem. 124 (2006) 192-199.

[44] R. Mancinelli, A. Botti, F. Bruni, M.A. Ricci, A.K. Soper, Hydration of sodium, potassium, and chloride ions in solution and the concept of structure maker/breaker, J. Phys. Chem. B 111 (2007) 13570-13577.

[45] K.H. Michaelian, M. Moskovits, Tetrahedral Hydration of Ions in Solution, Nature 273 (1978) 135-136.

[46] W.W. Rudolph, D. Fischer, G. Irmer, Vibrational spectroscopic studies and DFT calculations on NaCH3CO2(aq) and CH3COOH(aq), Dalton Trans. 43 (2014) 3174-3185.

[47] J.D.C. Craig, Raman spectroscopic and calculated vibrational wavenumbers of anion hydrates, J. Raman Spectrosc. 33 (2002) 191-196.

Highlights

- Polarization resolved ultrafast optical Kerr effect resolves previously unidentified modes in electrolyte solutions.
- Vibrational mode of Na^+ solvation shell observed.
- Enhancement effect of OH^- on water low frequency Raman spectrum observed.
- The K^+ solvation shell has too weak a signal to be resolved.